AIAA JOURNAL
Vol. 36, No. 10, October 1998

Axisymmetric Breakdown of a Q-Vortex in a Pipe

Z. Rusak,* C. H. Whiting,† and S. Wang‡
Rensselaer Polytechnic Institute, Troy, New York 12180-3590

Necessary and sufficient conditions for the axisymmetric breakdown of a Q-vortex in a pipe are presented. These unique calculations are guided by a recent rigorous theoretical approach on this subject (Wang, S., and Rusak, Z., "The Dynamics of a Swirling Flow in a Pipe and Transition to Axisymmetric Vortex Breakdown," *Journal of Fluid Mechanics*, Vol. 340, 1997, pp. 177–223). The fundamental characteristics that lead to vortex instability and breakdown in high-Reynolds-number swirling flows are computed from the solutions of a single, nonlinear, reduced-order, ordinary differential equation, representing a columnar flow problem. The breakdown criteria for the Q-vortex for various core radii and jet/wake axial flow profiles are described. Results show good agreement with available experimental data of axisymmetric breakdown in swirling flows in a pipe. The correlation between the present results and other criteria for vortex breakdown is also discussed.

Nomenclature

E	= flow force functional; Eq. (6)
$\boldsymbol{E}$	= energy functional; Eq. (4)
H	= total head function
I	= extended circulation function, $K^2/2$
K	= circulation function, rv
K_0	= inlet circulation function
p	= pressure
Re	= Reynolds number
Ro	= Rossby number
r	= radial distance from vortex axis
r_b	= breakdown zone radius
r_c	= vortex core radius
r_t	= pipe radius
u	= radial speed, $-\psi_x/r$
v	= circumferential speed
w	= axial speed, ψ_y
x	= axial distance, scaled with r_t
x_0	= pipe length, scaled with r_t
y	= $r^2/2$
y_b	= separation zone size, $r_b^2/2$
α_0, β_0	= helix angles for velocity and vorticity vectors
β	= vortex core radius parameter; Eq. (1)
δ	= jet/wake parameter; Eq. (1)
ρ	= density
ϕ	= eigenfunction; Eq. (7)
ψ	= stream function
Ω	= angular speed at vortex centerline, $\omega\beta$
ω	= vortex swirl ratio
ω_B	= Benjamin[6] critical swirl ratio
ω_0	= threshold critical swirl ratio
ω_1	= critical swirl ratio
ω^*	= threshold swirl ratio for columnar problem (5)

Subscripts

exp	= experimental
g	= partial differential equation (2) global minimizer
max	= maximal value
s	= ordinary differential equation (5) global minimizer
th	= theoretical
x, y	= derivative with x or y

Presented as Paper 97-0441 at the AIAA 35th Aerospace Sciences Meeting, Reno, NV, Jan. 6–9, 1997; received July 10, 1997; revision received May 1, 1998; accepted for publication May 23, 1998.

*Associate Professor, Department of Mechanical Engineering, Aeronautical Engineering and Mechanics. Senior Member AIAA.

†Graduate Student, Department of Mechanical Engineering, Aeronautical Engineering and Mechanics.

‡Postdoctoral Associate, Department of Mechanical Engineering, Aeronautical Engineering and Mechanics.

Introduction

THE breakdown of vortex cores in a pipe has become the topic of many studies in recent years. A significant and abrupt change in the vortex structure occurs when the swirl ratio (the ratio of maximum circumferential to axial speeds) of the incoming flow is above a certain value.[1–4] For combustion with swirl, vortex breakdown may help in flame stabilization and increase the combustion efficiency. Investigation of swirling flows in a pipe may also identify basic mechanisms of vortex destabilization and help to predict the onset of breakdown in aerodynamic problems such as around swept wings operating at high angles of attack. Several review papers on the subject show that vortex breakdown is still considered a basic, largely unexplained process with a variety of technological applications and scientific interests.[1–5]

Theoretical analyses of vortex breakdown concentrated on the axisymmetric case. Several explanations were proposed: the critical state concept,[6] the solitary trapped-wave approach,[7,8] the special state of a semi-infinite stagnation zone,[9] the analogy to boundary-layer separation,[1,10] the nature of swirling flow states in a diverging pipe,[11] and the appearance of hydrodynamic instabilities.[12,13] Some of the approaches show a possible relationship between the axisymmetric breakdown and the critical state concept.[6] However, the relations are not complete from either the theoretical standpoint or the application of the ideas to real flows in pipes or around wings. Moreover, normal-mode stability analyses[12,13] show no clear relation with the breakdown process.[3]

A variety of numerical studies were also carried out to simulate vortex breakdown.[14–19] They demonstrated that axisymmetric breakdown solutions may be found and showed some similarity with the physical situation but did not clarify the mechanism leading to this complicated process. In an effort to further understand the phenomenon, Beran and Culick[20] constructed various branches of numerical solutions of axisymmetric swirling flows in a pipe. The stability characteristics of these solutions have recently been studied.[21,22] These works provide an important insight into the breakdown process, specifically, with regard to the possible relationship between the flows stability and their breakdown that was not described in any of the theoretical approaches.[6–13]

Using the results from experimental data[2–4] and numerical simulations,[14–18] Spall et al.[23] suggested a criterion for the breakdown of vortex flows in terms of the flow Rossby number $Ro = w_c/r_c\Omega$. Here, r_c is the radial distance from the vortex axis of the maximum swirl velocity, Ω is the angular speed at the axis, and w_c is the axial speed at r_c. They found that, for flows with Reynolds numbers (based on w_c and r_c) greater than 100, vortex breakdown occurs when $Ro < 0.65$. This empirical criterion indicates that the appearance of

breakdown is probably related to global dynamical conditions and is not strongly affected by small viscosity or turbulence.

In another inviscid approach, Brown and Lopez[24] proposed a positive feedback mechanism between the divergence of the stream function surfaces near the vortex axis and the generation of negative azimuthal vorticity that leads to the formation of a free stagnation point. The mechanism relates between the helix angles α_0 and β_0 for the velocity and vorticity vectors at some upstream station. A stagnation point appears only when $\alpha_0 > \beta_0$. This condition is equivalent to the requirement $H' > 0$ near the vortex axis,[25] where H' is the derivative of the total head function with the stream function. It means that a stagnation point appears along the centerline only when the total head is minimal at the axis.

However, the mechanism[24] is only a necessary process for the appearance of a breakdown point but not sufficient. It can be shown that in certain vortex flows that definitely satisfy the Brown and Lopez[24] criterion breakdown states may appear, but they are unstable and convected out of the pipe, and the flow returns to a near-columnar state. In the study of vortex breakdown we are also interested in the critical conditions where the breakdown states are both steady and stable, and those are not described by the Brown and Lopez[24] mechanism and criterion.

The experimental studies[2–4] also show that swirling flows entering a pipe are characterized by a circumferential velocity component v, with a solid-body rotation near the centerline and a decay of swirl outside the rotational core, and by a jet profile for the axial velocity w. These vortex flows may be described by the Q-vortex model[2,4]

$$v(r) = (\omega/r)\left(1 - e^{-\beta r^2}\right), \qquad w(r) = 1 + \delta e^{-\beta r^2} \tag{1}$$

where β is related to the ratio of vortex core radius over pipe radius $r_c/r_t = 1.12/\sqrt{\beta}$. The parameter δ represents the nature of the axial speed profile; when $\delta > 0$, the axial flow has a jet-like profile, and when $\delta < 0$, it has a wake-like profile. In most of the pipe flows, $\delta > 0$ at the pipe inlet. The Q-vortex model can also describe the trailing vortices behind finite wings or the tip vortices of rotating blades, where $\delta < 0$, or approximate the leading-edge vortices above swept wings, where typically $\delta > 1$. Despite being a basic model of great interest in a variety of applications, the breakdown characteristics of the Q-vortex were not studied in previous works. One of the reasons for this may be the absence, until recently, of a general theoretical method to predict breakdown.

Recently, Wang and Rusak[26] and Rusak and Wang[27] have presented a novel theory that describes the axisymmetric vortex breakdown process. The approach is based on a rigorous study of the dynamics of swirling flows in a finite-length straight pipe as given by the axisymmetric and unsteady Euler equations. Certain boundary conditions that may reflect the physical situation in experiments[2–5,28] are used. The analysis studies the growth rate of an initial perturbation as it relates to the special stability characteristics found by Wang and Rusak,[29,30] as well as the relation of the flow time-asymptotic behavior to steady-state solutions.[26] There exist two critical swirl ratios of the incoming flow to the pipe, ω_0 and ω_1, where $\omega_0 < \omega_1$. Columnar flows with a swirl ratio less than the threshold level ω_0 are unconditionally stable to any axisymmetric disturbance. In the range $\omega_0 < \omega < \omega_1$, the flow may evolve into one of two steady states, depending on the size of the initial disturbances. When disturbances are sufficiently small, they decay in time and the flow returns to be columnar, but, when disturbances are large, they grow and evolve into a large and steady, semi-infinite stagnation zone, similar to the breakdown states found in very-high-Reynolds-number flows.[5] When $\omega > \omega_1$, any initial disturbance grows and evolves into a breakdown zone.

These special stability characteristics are related to the propagation upstream of both small- and large-amplitude disturbances and their interaction with the flow conditions downstream of the vortex generator. The disturbances tend to propagate upstream with a speed that increases with ω. When $\omega < \omega_1$, small disturbances are convected by the axial flow out of the pipe, and the columnar flow is, therefore, stable. However, when $\omega > \omega_1$, small disturbances tend to move upstream. Because the flow out of the vortex generator at steady operation is fixed, the disturbances cannot move through it. They become trapped, grow, and stabilize as a large and steady stagnation zone. These large-amplitude zones also tend to move upstream as ω changes, but, when $\omega < \omega_0$, they are convected by the axial flow out of the pipe, and the flow returns to be columnar.

These results clarify the mechanism leading to the axisymmetric vortex breakdown in high-Reynolds-number flows. As the incoming swirl ratio is increased above ω_0 and is near or above ω_1, the columnar vortex loses its stability to axisymmetric disturbances and evolves into a breakdown state. The theory explains the sudden and abrupt nature of the process, specifically around ω_0, where a large separation zone may suddenly appear in the flow as swirl increases. It also clarifies the role of the critical state at ω_1, where a columnar vortex becomes unstable as swirl increases, and that at ω_0, where axisymmetric breakdown states become unstable as swirl decreases. Therefore, ω_0 is a threshold level for breakdown states, and $\omega > \omega_0$ is a necessary condition for a steady and stable axisymmetric breakdown; $\omega > \omega_1$ is a sufficient condition for breakdown.

Analysis of the effect of slight viscosity on the flow dynamics shows that when the Reynolds number *Re* is sufficiently high the inviscid instability/transition mechanism is dominant.[31] This dynamical behavior matches the simulations[21,22] for high-Reynolds-number laminar flows. The establishment of long and nearly stagnant breakdown zones as the Reynolds number increases is also found in the simulations. However, when the Reynolds number is less than a certain value, both the analysis[31] and simulations[19–22] show that the instability mechanism disappears and breakdown develops as a disturbance that gradually grows with the increase in the incoming swirl ratio. Also, the simulations[21] demonstrate that the separation zone becomes a closed bubble with an internal flow structure as the Reynolds number decreases, similar to the states found in laminar flow experiments.[2–5] Yet, the threshold swirl for breakdown does not change significantly with Reynolds number,[21] and the inviscid value ω_0 may provide a good estimate for the first appearance of breakdown in low- and high-Reynolds-number flows.

Rusak and Wang[27] demonstrated that the theory[26] unifies the previous theoretical approaches[6–13] and numerical studies[19–22] and fills the relations between them. It provides, for the first time, a general and simple framework in which computations of conditions for vortex breakdown can be conducted and can be applied to any relevant vortex flow including experimental profiles. A brief review of the methods to compute the critical swirl ratios is described in the following sections. The methods are extended to calculate the necessary and sufficient conditions for the axisymmetric breakdown of a Q-vortex in a pipe.

From a computational point of view, the analysis of the Q-vortex model (1) is much more complicated than the analyses of the Rankine or the Burgers vortex models described in Refs. 26 and 32. Unlike the later models, in the case of the Q-vortex the axial velocity profile (1) cannot be inverted in a direct analytical method to give the function $y(\psi)$ needed later in Eqs. (10). This function has to be computed numerically as part of the computational process of solving the differential equations and calculating the critical swirls ω_0 and ω_1 (see Ref. 33). Also, the results for the Rankine[26] and Burgers[32] vortices demonstrate the relation between the theory[26] and the numerical simulations of vortex breakdown but cannot be directly compared with experimental data. The results for the Q-vortex model presented in this paper are relevant for the experimental flows described in Refs. 3 and 34 and demonstrate the relation between the theory[26] and the experiments.

It should be clarified that the breakdown of high-Reynolds-number swirling flows is a large-scale change in the flow structure. Therefore, it is expected, as well as demonstrated in various experimental,[2–4] computational,[19–22] and theoretical[31] studies, that the effect of small viscosity on the flow behavior is quite limited, and the breakdown process is primarily governed by the convective effects. This comment may also be relevant to the mean flow behavior of very-high-Reynolds-number turbulent flows. Notice, again, the similarity between the open separation zone predicted by the theory and the open breakdown zones found recently by Sarpkaya[5] in turbulent swirling flows. Therefore, it is expected that the present study provides relevant results for high-Reynolds-number swirling flows, including turbulent flows of practical applications.

Only a small number of experimental studies on vortex breakdown in pipes[2,3,33] provide detailed inlet flow profiles that can be analyzed by the theory. Most of the experimental reports provide only external conditions with no detailed flow profiles near the vortex core, which dominate the breakdown characteristics. The present results can guide future experimental studies on vortex breakdown.

Method to Compute ω_0

The method to compute ω_0 results from the nature of solutions of the Squire–Long equation (SLE) (resulting from the axisymmetric, steady-state Euler equations)

$$\psi_{yy} + \psi_{xx}/2y = H'(\psi) - I'(\psi)/2y \tag{2}$$

with boundary conditions

$$\psi(x, 0) = 0, \qquad \psi\left(x, \tfrac{1}{2}\right) = \psi_0\left(\tfrac{1}{2}\right)$$
$$\psi(0, y) = \psi_0(y), \qquad K(0, y) = \omega K_0(y), \qquad \psi_x(x_0, y) = 0 \tag{3}$$

Here, $y = r^2/2$, $\psi(x, y)$ is the stream function and $\psi_0(y)$ and $\omega K_0(y)$ are the inlet stream function and circulation profiles. $H = p/\rho + (u^2 + w^2 + v^2)/2$ is the total head function, and $I = K^2/2$ is the extended circulation, and both are functions of ψ only. Solutions of the SLE correspond to the extremum points of the following energy functional[9]:

$$\boldsymbol{E}(\psi) = \int_0^{x_0} \int_0^{\frac{1}{2}} \left[\frac{\psi_y^2}{2} + \frac{\psi_x^2}{4y} + H(\psi) - \frac{I(\psi)}{2y} \right] \mathrm{d}y\, \mathrm{d}x \tag{4}$$

It has been shown[26] that the solution $\psi_g(x, y)$ that globally minimizes $\boldsymbol{E}(\psi)$ is dominated by the solution $\psi_s(y)$ of the columnar, ordinary differential equation (ODE) problem

$$\psi_{yy} = H'(\psi) - I'(\psi)/2y, \qquad \psi(0) = 0, \qquad \psi\left(\tfrac{1}{2}\right) = \psi_0\left(\tfrac{1}{2}\right) \tag{5}$$

that globally minimizes the variational flow-force functional[6]

$$E(\psi) = \int_0^{\frac{1}{2}} \left[\frac{\psi_y^2}{2} + H(\psi) - \frac{I(\psi)}{2y} \right] \mathrm{d}y \tag{6}$$

There exists a certain swirl level ω_0. When $\omega < \omega_0$, the global minimizer solution of the ODE (5) is the base inlet flow, $\psi_s(y) = \psi_0(y)$, which implies that the global minimizer solution of the SLE (2) is the columnar flow $\psi_g(x, y) = \psi_0(y)$. However, when $\omega > \omega_0$, the global minimizer solution $\psi_s(y)$ of the ODE (5) is quite different from $\psi_0(y)$, with $E[\psi_s(y)] < E[\psi_0(y)]$. This solution contains a separation region in the domain $0 \le y \le y_b$. Then, the global minimizer solution of the SLE (2) describes a vortex breakdown state, which is a transition along the pipe axis from an inlet state $\psi_g(0, y) = \psi_0(y)$ to a lower energy outlet state $\psi_g(x_0, y) = \psi_s(y)$. Conservation of momentum considerations show that when $\omega > \omega_0$ the difference in flow force

$$E[\psi_0(y)] - E[\psi_s(y)] = \int_0^{\frac{1}{2}} \frac{\psi_x^2(0, y)}{2y}\, \mathrm{d}y$$

creates a radial flow across the pipe inlet to develop the separation zone.

The solution that globally minimizes $E(\psi)$ depends on the choice of a continuation model in the separation zone. The inviscid[32] and viscous[21] simulations show that, starting from initial conditions of a perturbed columnar state, the flow always evolves with no reversed flow along the outlet or inside the pipe domain and a stagnation zone naturally appears when $\omega > \omega_0$ and as time tends to infinity. It, therefore, seems plausible to choose a stagnation model in the search of solutions of SLE (2) and ODE (5).

To compute ω_0 it is, therefore, necessary to find all of the solutions of the ODE (5) for a given ω, including solutions with a stagnation zone around the centerline. Then, the integral $E(\psi)$ [Eq. (6)] is computed for each solution and compared with the integral $E(\psi_0)$ of the base inlet state with the same ω. The swirl level, where $E(\psi)$ is no longer minimized by the base inlet vortex state or where there exists another solution $\psi_s(y)$ with $E[\psi_s(y)] = E[\psi_0(y)]$, is the bifurcation swirl ω_0, which is the threshold level for the appearance of steady and stable axisymmetric vortex breakdown states.

Method to Compute ω_1

Wang and Rusak[26] showed that the critical swirl ratio ω_1 for a swirling flow in a finite-length pipe is the first eigenvalue of the linearized problem resulting from Eq. (2),

$$\phi_{yy} - \left(\frac{\pi^2}{8x_0^2 y} + \frac{\psi_{0yyy}}{\psi_{0y}} - \omega^2 \frac{K_0 K_{0y}}{2y^2 \psi_{0y}^2} \right) \phi = 0$$
$$\phi(0) = 0, \qquad \phi\left(\tfrac{1}{2}\right) = 0 \tag{7}$$

For a swirling flow in a long pipe, where $x_0 \gg 1$, this critical level approaches Benjamin's[6] critical swirl ω_B that is found from the linearized columnar problem resulting from Eq. (5),

$$\phi_{yy} - \left(\frac{\psi_{0yyy}}{\psi_{0y}} - \omega^2 \frac{K_0 K_{0y}}{2y^2 \psi_{0y}^2} \right) \phi = 0$$
$$\phi(0) = 0, \qquad \phi\left(\tfrac{1}{2}\right) = 0 \tag{8}$$

For most of the practical cases the pipe is considered sufficiently long, and ω_1 is approximated by ω_B.

Conditions for the Axisymmetric Breakdown of a Q-Vortex

In the case of the Q-vortex model (1), the following relations are found:

$$\psi_0(y) = \frac{\delta}{2\beta} + y - \frac{\delta}{2\beta} e^{-2\beta y}, \qquad \omega K_0(y) = \omega(1 - e^{-2\beta y}) \tag{9}$$

Therefore, it can be shown that

$$I'(\psi) = 2\beta\omega^2 \left(1 - e^{-2\beta y(\psi)}\right) e^{-2\beta y(\psi)}$$
$$H'(\psi) = \frac{I'[y(\psi)]}{2y(\psi)} - 2\beta\delta\, e^{-2\beta y(\psi)} \tag{10}$$

where the function $y(\psi)$ can be computed from Eq. (9) for every β and δ. For fixed values of β, δ, and ω, Eq. (5) is numerically integrated using a standard differential equation solver from the NAG Fortran routines. We look for solutions of Eq. (5) where, specifically, $0 \le \psi \le \frac{1}{2}$ in the domain $0 \le y \le \frac{1}{2}$ and a stagnation region with $\psi = 0$ may appear in the solution in a finite region $0 \le y \le y_b$ and where $\psi(y_b) = \psi_y(y_b) = 0$. Equation (5) together with these conditions at $y = y_b$ completely specifies a free boundary value problem from which the size of the stagnation zone y_b may be determined as a function of the swirl level. Details of the computational methods to solve this problem are given in Ref. 33. It is important to notice that there exist other solutions of Eq. (5) with reversed flow regions, where $\psi < 0$ in a certain region of the domain $(0, \frac{1}{2})$ when a different continuation model is used. However, those are not relevant to the steady-state solutions of the time-dependent inviscid flow problem.

Typical solutions of Eq. (5) for various values of ω are presented in Figs. 1a and 1b for $\beta = 4.0$ ($r_c/r_t = 0.56$) with $\delta = 1.0$ and $\delta = -0.5$, respectively. Computations for other values of β and δ show similar results. We find that, for any β and δ, in addition to the base solution $\psi_0(y)$ there exist two other types of solutions that meet the preceding requirements: type I, where $\psi(0) = 0$ but $\psi_y(0) > 0$, and type II, where $\psi(0) = 0$ in the domain $0 \le y \le y_b$ (stagnation region) and $\psi_y(y_b) = 0$. We also find that there exists a certain level of swirl $\omega^*(\beta, \delta)$, where for $\omega < \omega^*(\beta, \delta)$ only the base solution exists. The swirl level $\omega^*(\beta, \delta)$ is a bifurcation point of solutions of Eq. (5). At $\omega = \omega^*(\beta, \delta)$, we find two solutions: One is the base solution, and the other is a special solution of type II. When ω is slightly greater than $\omega^*(\beta, \delta)$, three solutions are found: One is the base solution, and the other two, $\psi_1(y; \omega, \delta)$ and $\psi_2(y; \omega, \delta)$, have large and small stagnation regions, respectively. When ω is further increased, the branch of $\psi_1(y; \omega, \delta)$ solutions of type II describes

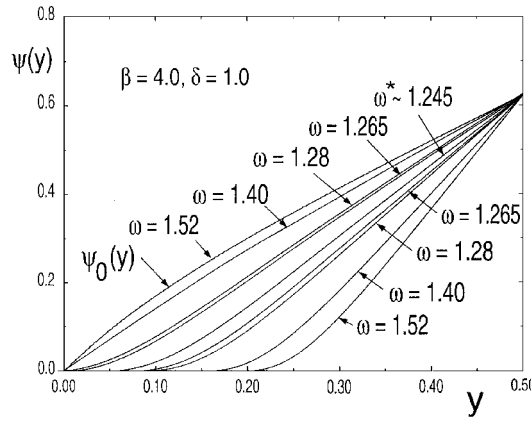

Fig. 1a Solutions of Eq. (6) when $\beta = 4.0$ and $\delta = 1.0$.

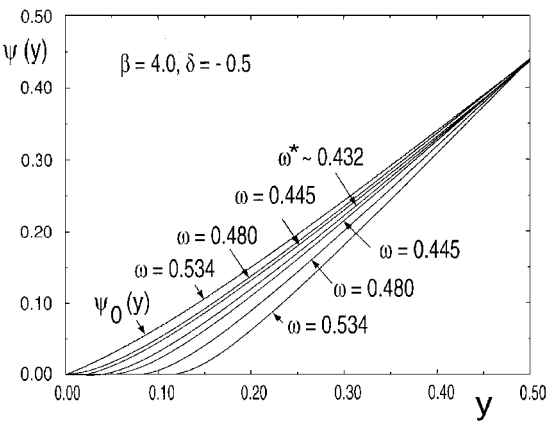

Fig. 1b Solutions of Eq. (6) when $\beta = 4.0$ and $\delta = -0.5$.

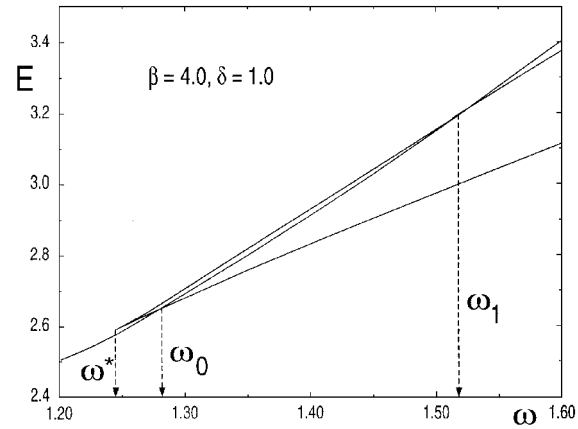

Fig. 2a Bifurcation diagram of solutions of Eq. (6) for $\beta = 4.0$ and $\delta = 1.0$.

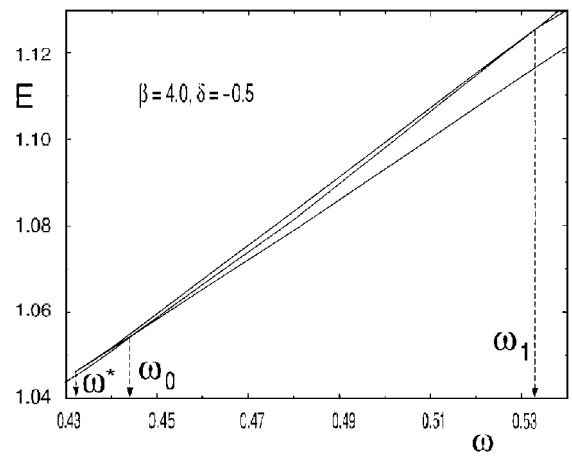

Fig. 2b Bifurcation diagram of solutions of Eq. (6) for $\beta = 4.0$ and $\delta = -0.5$.

larger stagnation zones, whereas the branch of $\psi_2(y; \omega, \delta)$ solutions with the small stagnation zone changes naturally into solutions of type I. The latter branch approaches the trivial solution as ω approaches the critical bifurcation point $\omega_B(\beta, \delta)$, discussed earlier.

For each one of the solutions of the ODE (5), E [as given by Eq. (6)] can be calculated (see Ref. 33 for more details of these computations). Typical results are shown in the bifurcation diagrams (Figs. 2a and 2b) for the case $\beta = 4.0$ with $\delta = 1.0$ and -0.5, respectively. Similar bifurcation diagrams can be constructed for any value of β and δ. It can be seen that there exists a certain level of swirl defined as ω_0 for which $E(\psi_1) = E(\psi_0)$ and across which the solution that minimizes $E(\psi)$ is changed. When $\omega^* < \omega < \omega_0$, we find $E(\psi_2) > E(\psi_1) > E(\psi_0)$, whereas for $\omega_0 < \omega < \omega_B$, we find $E(\psi_2) > E(\psi_0) > E(\psi_1)$. It can be concluded that $\psi_0(y)$ is a global minimizer of $E(\psi)$, when $\omega < \omega_0$, whereas $\psi_1(y; \omega, \delta)$ is a global minimizer of $E(\psi)$, when $\omega > \omega_0$. It can also be shown that, in the region $\omega_0 < \omega < \omega_B$, the solution $\psi_2(y; \omega, \delta)$ is a min–max point of $E(\psi)$. When $\omega > \omega_B$, we have $E(\psi_0) > E(\psi_2) > E(\psi_1)$, which implies that in this range the base solution ψ_0 is a min–max point and the solution ψ_2 is a local minimizer of $E(\psi)$.

These results show behavior similar to the theoretical discussion on the Rankine vortex model described in Ref. 26 and on Burgers' vortex [where in Eq. (1) $\delta = 0$] described in Ref. 32.

The bifurcation diagrams in Figs. 2a and 2b can now be used to describe the steady-state solutions of SLE (2) with conditions (3). When $\omega < \omega_0$, only one steady-state solution will develop that describes a columnar flow. When $\omega_0 < \omega < \omega_1$, we may find three steady-state solutions. One describes a columnar flow and is a local minimizer of $\boldsymbol{E}(\psi)$. The second describes a swirling flow with a localized stagnation zone that disappears as ω is increased toward ω_1 and is a min–max point of $\boldsymbol{E}(\psi)$. The third solution describes a swirling flow around a stagnation zone and is the global minimizer of $\boldsymbol{E}(\psi)$. The size of the stagnation region in the latter solution corresponds to that of the separation zone y_b of the ODE solution $\psi_1(y; \omega)$ and increases as ω is increased.

We can now conclude, through considerations of the stability analyses of Wang and Rusak,[29,30] that only the local and global minimizer solutions are linearly stable to axisymmetric disturbances, whereas the min–max solutions are unstable. Therefore, with regard to solutions of the problem defined by Eqs. (2), we find that, when $\omega < \omega_0$, only one-steady state solution that is a columnar swirling flow can develop. When $\omega_0 < \omega < \omega_1$, two steady-state solutions may develop, depending on the initial disturbances to the base flow. When $\omega > \omega_1$, we find that the flow will always develop into the steady breakdown state described by the global minimizer solution of Eq. (2). We can infer that steady breakdown solutions can be found only when $\omega > \omega_0$, and when $\omega > \omega_1$, such breakdown solutions will always develop.

For the Q-vortex model, the values of the swirl ratios $v_{\max}/w_0$ [where $v_{\max} = v(r = r_c) = 0.638\omega\sqrt{\beta}$ and $w_0 = 1 + \delta$ is the axial speed at the centerline] that correspond to the threshold swirl ω_0 and the critical swirl ω_1 as function of the ratio of vortex core radius over pipe radius, $r_c/r_t = 1.12/\sqrt{\beta}$, are presented in Figs. 3a and 3b for $\delta = 1.0$ and -0.5, respectively. It can be seen that as the vortex core radius over pipe radius is reduced the threshold and critical swirl ratios for breakdown also decrease but the difference between them increases. Notice that finite limit values of the the two special swirl ratios are found when r_c/r_t approaches zero (or β tends to infinity). These limit swirl ratios may be used as breakdown criteria for a free Q-vortex in an unbounded domain.

The values of the swirl ratio $v_{\max}/w_0$ that correspond to ω_0 and ω_1 as function of the axial flow jet/wake parameter in the range $-1 < \delta \leq 1$ are presented in Figs. 4a and 4b for $\beta = 4.0$ ($r_c/r_t = 0.56$) and $\beta = 32.0$ ($r_c/r_t = 0.20$), respectively. It can be seen that, as δ increases, the swirl ratios $v_{\max}/w_0$ approach constant values, which also depend on β. For a small core vortex these threshold swirl ratios approach a value about 0.6 as δ increases. This limit swirl level may be used as a breakdown criterion for a free vortex with a

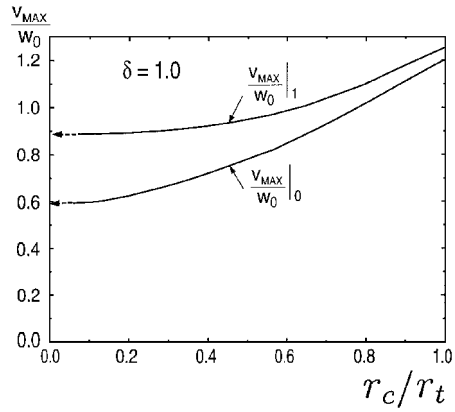

Fig. 3a Breakdown criteria for a Q-vortex when $\delta = 1.0$.

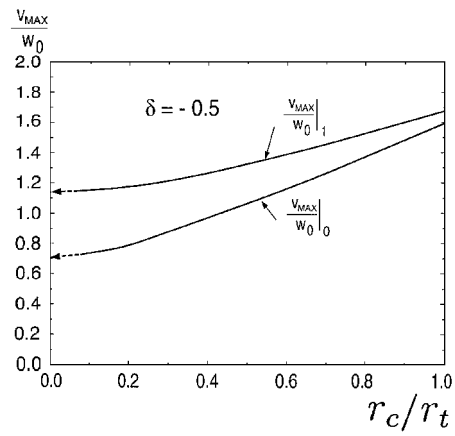

Fig. 3b Breakdown criteria for a Q-vortex when $\delta = -0.5$.

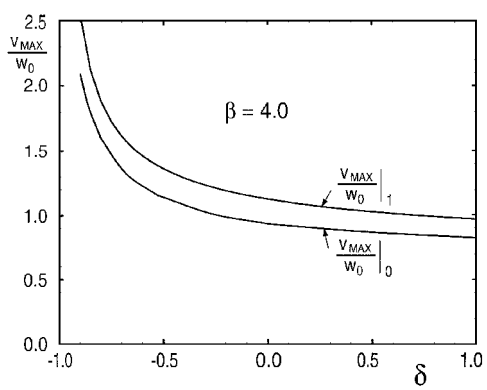

Fig. 4a Breakdown criteria for a Q-vortex when $\beta = 4.0$.

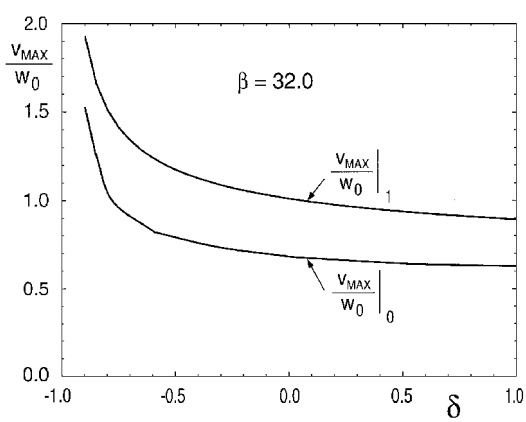

Fig. 4b Breakdown criteria for a Q-vortex when $\beta = 32.0$.

strong axial jet, such as the leading-edge vortices above swept wings. When $\delta < -0.6$, the threshold swirl ratio for breakdown increases significantly. However, in such axial shear flows of strong wake-like nature, other effects may appear, and their interaction with the swirl may result in additional interesting phenomena that should also be carefully studied but are beyond the scope of this paper.

Figures 3 and 4 provide for the first time guiding criteria for the appearance of the axisymmetric breakdown in a Q-vortex entering a pipe.

Comparisons with Experimental Data and Other Criteria

The described methodology is now used to compare the theoretical predictions for the axisymmetric vortex breakdown with experimental results for Q-vortices reported by Garg and Leibovich[34] and Leibovich.[3] For each of the Q-vortices reported in these experiments, the corresponding values of β and δ that characterize those profiles may be computed. Using these values, we compute the critical swirl levels $\omega_0(\beta, \delta)$ and $\omega_1(\beta, \delta)$. The results are summarized in Table 1. It can be seen that, for all incoming experimental flows, where axisymmetric breakdown occurred, the swirl parameter in the experiments ω_{exp} is always between the respective ω_0 and ω_1 and usually slightly above ω_0, thus satisfying the necessary condition for the axisymmetric breakdown.

For each one of the experimental profiles, the relevant breakdown solution of the ODE (5) was also computed. The resulting stagnation zone size divided by the vortex core radius $[r_b/r_c]_{\text{th}}$ is compared with the experimental results of the vortex core expansions $[r_b/r_c]_{\text{exp}}$ as reported by Leibovich[3] (Table 1). A good agreement between the theoretical predictions and the experimental results is found in all cases. As can be expected, the present inviscid breakdown theory predicts slightly larger breakdown zones. It is expected that viscous effects result in the creation of an internal recirculation flow in the breakdown zone through the diffusion of momentum and energy from the outer flow into the separation zone, thus slightly reducing the size of the breakdown zone predicted by the inviscid analysis.

Figure 5 describes the results according to our theory in terms of the Rossby number Ro (Ref. 23). For a Q-vortex, we find that $Ro\,(\omega; \beta, \delta) = (1 + \delta e^{-1.12^2})/1.12\omega\sqrt{\beta}$. Lines corresponding to $Ro\,[\omega_0(\beta, \delta)]$ are shown for $\beta = 4.0$ $(r_c/r_t = 0.56)$ and $\beta = 32.0$ $(r_c/r_t = 0.2)$. Steady axisymmetric breakdown states can occur when $Ro < Ro\,[\omega_0(\beta, \delta)]$. Also shown in Fig. 5 are lines for the criterion of Spall et al.,[23] $Ro < 0.65$, and the criteria using Rossby number according to Brown and Lopez,[24] $Ro < \sqrt{(1 - 1/e)(1 + \delta e^{-1.12^2})/\{1.12\sqrt{[\delta(1 + \delta/e)]}\}}$, and according to Rusak,[25] $Ro < (1 + \delta e^{-1.12^2})/\{1.12\sqrt{[\delta(1 + \delta)]}\}$.

Table 1 Comparison of the theoretical predictions with the experimental results of Garg and Leibovich[34] and Leibovich[3]

$\delta = W_2/W_1$	$\beta = \alpha r_t^2$	$\omega_{\text{exp}} = q\lvert\delta\rvert/W_1$	ω_0	ω_1	$r_b/r_c\rvert_{\text{exp}}$	$r_b/r_c\rvert_{\text{th}}$
1.58	32.4	0.44	0.43	0.61	2.5	2.8
1.40	31.8	0.41	0.40	0.58	2.0	2.3
1.48	56.2	0.32	0.31	0.45	2.8	3.0

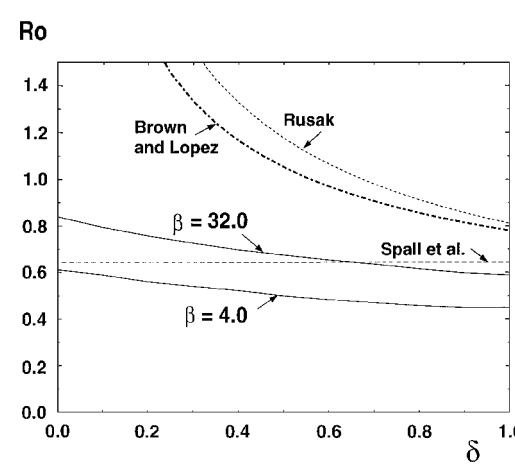

Fig. 5 Breakdown criteria for a Q-vortex according to various criteria.

Figure 5 shows that Brown and Lopez[24] and Rusak[25] criteria predict the possible existence of breakdown states at much higher Rossby numbers than those predicted by the present theory, specifically when the axial jet parameter δ is small, $\delta < 0.5$. Therefore, it is clear that the present results always satisfy the necessary conditions of Brown and Lopez[24] and Rusak[25] criteria. Moreover, according to our theory,[26] it is concluded that the breakdown states that may be found in the range of Rossby number between the present calculations and the Rusak[25] line are unstable to axisymmetric disturbances and will be convected out from the pipe domain after some time. From this perspective, both Brown and Lopez[24] and Rusak[25] criteria overpredict the range for the appearance of steady and stable axisymmetric breakdown states.

Figure 5 also shows that the Spall et al.[23] criterion is relevant in some range of $\delta > 0.5$. However, according to the present results, when the vortical core radius of the vortex is small, $r_c/r_t < 0.25$ (or $\beta > 25.0$) and $\delta < 0.3$, we predict that steady breakdown states of the Q-vortex can be found even when $Ro > 0.65$. From this perspective the Rossby number criterion defined by Spall et al.[23] may not be sufficient to describe all cases of steady and stable axisymmetric breakdown states in a swirling flow in a pipe. We, therefore, recommend use of the swirl ratio criterion $v_{\max}/w_0 > (v_{\max}/w_0)_0(\beta, \delta)$ described earlier as the guiding criterion for the axisymmetric breakdown of a Q-vortex in a pipe.

Summary

This paper presents numerical calculations of the necessary and sufficient conditions for the axisymmetric breakdown of a Q-vortex in a pipe. These unique calculations are guided by a recent rigorous theory on this subject by Wang and Rusak[26] and Rusak and Wang.[27] We demonstrate that the fundamental characteristics that lead to vortex instability and breakdown in high-Reynolds-number swirling flows are computed from the solutions of a single, nonlinear, reduced-order ODE, representing a columnar flow problem. The breakdown criteria for the Q-vortex for various core radii and jet/wake axial flow profiles are described. Results show good agreement with available experimental data of swirling flows in a pipe.

The correlation between the present results and other criteria for vortex breakdown is discussed. It is shown that both Brown and Lopez[24] and Rusak[25] criteria overpredict the range for the appearance of steady and stable axisymmetric breakdown states. It is also demonstrated that the Rossby number criterion defined by Spall et al.[23] may not be sufficient to describe all cases of steady and stable axisymmetric breakdown states in a swirling flow in a pipe.

We propose use of the swirl ratio criterion $(v_{\max}/w_0) > (v_{\max}/w_0)_0(\beta, \delta)$ described in Figs. 3 and 4 as the guiding criterion for the axisymmetric breakdown of a Q-vortex in a pipe. Also, in the limit of a small core radius (or large β), the present results may provide the threshold swirl ratio for the breakdown of a free Q-vortex or a partially bounded vortex such as the leading edge vortices above delta wings.

Acknowledgments

This research was carried out with the support of the National Science Foundation under Grant CTS-9310181. The first author would also like to thank the United States–Israel Binational Science Foundation for their partial support of this research under Grant 94-00245/1.

References

[1]Hall, M. G., "Vortex Breakdown," *Annual Review of Fluid Mechanics*, Vol. 4, 1972, pp. 195–217.

[2]Leibovich, S., "The Structure of Vortex Breakdown," *Annual Review of Fluid Mechanics*, Vol. 10, 1978, pp. 221–246.

[3]Leibovich, S., "Vortex Stability and Breakdown: Survey and Extension," *AIAA Journal*, Vol. 22, No. 9, 1984, pp. 1192–1206.

[4]Escudier, M., "Vortex Breakdown: Observations and Explanations," *Progress in Aerospace Science*, Vol. 25, 1988, pp. 189–229.

[5]Sarpkaya, T., "Vortex Breakdown and Turbulence," AIAA Paper 95-0433, Jan. 1995.

[6]Benjamin, T. B., "Theory of the Vortex Breakdown Phenomenon," *Journal of Fluid Mechanics*, Vol. 14, 1962, pp. 593–629.

[7]Randall, J. D., and Leibovich, S., "The Critical State: A Trapped Wave Model of Vortex Breakdown," *Journal of Fluid Mechanics*, Vol. 58, 1973, pp. 495–515.

[8]Leibovich, S., and Kribus, A., "Large Amplitude Wavetrains and Solitary Waves in Vortices," *Journal of Fluid Mechanics*, Vol. 216, 1990, pp. 459–504.

[9]Keller, J. J., Egli, W., and Exley, J., "Force- and Loss-Free Transitions Between Flow States," *Journal of Applied Mathematics and Physics (ZAMP)*, Vol. 36, No. 6, 1985, pp. 854–889.

[10]Hall, M. G., "A New Approach to Vortex Breakdown," *Proceedings of the Heat Transfer and Fluid Mechanics Institute*, Univ. of California, San Diego, CA, 1967, pp. 319–340.

[11]Buntine, J. D., and Saffman, P. G., "Inviscid Swirling Flows and Vortex Breakdown," *Proceedings of the Royal Society of London A*, Vol. 449, 1995, pp. 139–153.

[12]Lessen, H., Singh, P. J., and Paillet, F., "The Stability of a Trailing Line Vortex, Part 1: Inviscid Theory," *Journal of Fluid Mechanics*, Vol. 63, 1974, pp. 753–763.

[13]Leibovich, S., and Stewartson, K., "A Sufficient Condition for the Instability of Columnar Vortices," *Journal of Fluid Mechanics*, Vol. 126, 1983, pp. 335–356.

[14]Grabowski, W. J., and Berger, S. A., "Solutions of the Navier–Stokes Equations for Vortex Breakdown," *Journal of Fluid Mechanics*, Vol. 73, No. 3, 1976, pp. 525–544.

[15]Krause, E., "Pressure Variation in Axially Symmetric Breakdown," *Proceedings of the Colloquium on Vortex Breakdown*, RWTH, Aachen, Germany, 1985, pp. 49–68.

[16]Hafez, M. M., and Salas, M. D., "Vortex Breakdown Simulation Based on Nonlinear Inviscid Model," *Studies of Vortex Dominated Flows*, edited by M. Y. Hussaini and M. D. Salas, Springer–Verlag, Berlin, 1985, pp. 76–83.

[17]Salas, M. D., and Kuruvila, G., "Vortex Breakdown Simulation: A Circumspect Study of the Steady, Laminar, Axisymmetric Model," *Computers and Fluids*, Vol. 17, No. 1, 1989, pp. 247–262.

[18]Spall, R. E., and Gatski, T. B., "A Computational Study of the Topology of Vortex Breakdown," *Proceedings of the Royal Society of London A*, Vol. 435, 1991, pp. 321–337.

[19]Darmofal, D. L., "Comparisons of Experimental and Numerical Results for Axisymmetric Vortex Breakdown in Pipes," *Computers and Fluids*, Vol. 25, No. 4, 1996, pp. 353–371.

[20]Beran, P. S., and Culick, F. E. C., "The Role of Non-Uniqueness in the Development of Vortex Breakdown in Tube," *Journal of Fluid Mechanics*, Vol. 242, 1992, pp. 491–527.

[21]Lopez, J. M., "On the Bifurcation Structure of Axisymmetric Vortex Breakdown in a Constricted Pipe," *Physics of Fluids*, Vol. 6, No. 11, 1994, pp. 3683–3693.

[22]Beran, P. S., "The Time-Asymptotic Behavior of Vortex Breakdown in Tubes," *Computers and Fluids Journal*, Vol. 23, No. 7, 1994, pp. 913–937.

[23]Spall, R. E., Gatski, T. B., and Grosch, C. E., "A Criterion for Vortex Breakdown," *Physics of Fluids*, Vol. 30, No. 11, 1987, pp. 3434–3440.

[24]Brown, G. L., and Lopez, J. M., "Axisymmetric Vortex Breakdown, Part 2: Physical Mechanisms," *Journal of Fluid Mechanics*, Vol. 221, 1990, pp. 553–576.

[25]Rusak, Z., "Swirling Flow Around a Breakdown Point," *Journal of Fluid Mechanics*, Vol. 323, 1996, pp. 79–105.

[26]Wang, S., and Rusak, Z., "The Dynamics of a Swirling Flow in a Pipe and Transition to Axisymmetric Vortex Breakdown," *Journal of Fluid Mechanics*, Vol. 340, 1997, pp. 177–223.

[27]Rusak, Z., and Wang, S., "Review of Theoretical Approaches to the Vortex Breakdown Phenomenon," AIAA Paper 96-2126, June 1996.

[28]Bruecker, C., and Althaus, W., "Study of Vortex Breakdown by Particle Tracking Velocimetry (PTV), Part 3: Time-Dependent Structure and Development of Breakdown Modes," *Experiments in Fluids*, Vol. 18, 1995, pp. 174–186.

[29]Wang, S., and Rusak, Z., "On the Stability of an Axisymmetric Rotating Flow in a Pipe," *Physics of Fluids*, Vol. 8, No. 4, 1996, pp. 1007–1016.

[30]Wang, S., and Rusak, Z., "On the Stability of Non-Columnar Swirling Flows," *Physics of Fluids*, Vol. 8, No. 4, 1996, pp. 1017–1023.

[31]Wang, S., and Rusak, Z., "The Effect of Slight Viscosity on Near Critical Swirling Flows," *Physics of Fluids*, Vol. 9, No. 7, 1997, pp. 1914–1927.

[32]Rusak, Z., Wang, S., and Whiting, C., "Numerical Computations of Axisymmetric Vortex Breakdown in a Pipe," AIAA Paper 96-0801, Jan. 1996.

[33]Whiting, C. H., "Analysis of the Vortex Breakdown Phenomenon," M.S. Thesis, Dept. of Mechanical Engineering, Rensselaer Polytechnic Inst., Troy, NY, May 1996.

[34]Garg, A. K., and Leibovich, S., "Spectral Characteristics of Vortex Breakdown," *Physics of Fluids*, Vol. 22, No. 11, 1979, pp. 2053–2064.

P. R. Bandyopadhyay
Associate Editor